

HIGHER FULLERENES FROM COAL AND THEIR FAVORABLE ISOMERIC STRUCTURES

J. S. QIU^{1*}, E. Osawa², H.M. Han¹, M. Yoshida², Y. Zhou¹, T. Mieno³

1. Carbon Research Laboratory, School of Chemical Engineering, Dalian University of Technology,
158 Zhongshan Road, P.O. Box 33, Dalian 116012, China

2. Dept. of Knowledge-based Information Engineering, Toyohashi University of Technology,
Toyohashi 441, Japan

3. Department of Physics, Shizuoka University, 836 Ooya, Japan

Introduction

Fullerenes represent a new carbon allotrope having a common structural feature of completely closed network consisting of essentially hexagons and pentagons. Its first member C_{60} was first discovered in 1985. An old theorem of geometry that twelve pentagons and any number of hexagonal rings form a closed solid, was immediately recalled to predict and to account for the exceptional stability of the fullerenes species, and this structural principle helped enormously to understand and expand the structural variation of fullerenes. The discovery of fullerenes triggered unprecedented vigorous research activities in the field of carbon science, which continued strong throughout the past decade, though at the moment the carbon nanotubes (CNTs), both multi-walled and single-walled, and other novel carbon nanomaterials are the most popular research targets. It is believed that fullerenes and CNTs will be potentially useful as novel materials in a number of fields including catalysts, rechargeable batteries, chemical reagents, superconductors, and composite materials.

Fullerenes can be prepared from different carbon sources by a number of processes such as laser ablation, the concentration of solar flux, resistive or inductive heating of a graphite rod, plasma jets, sputtering and ion beam evaporation, and flames. However, the carbon arc reactor is, at present, the most efficient and economically viable technique for the production of fullerenes. This process is also widely used for the preparation of nanotubes and other novel nanomaterials, although at different operating conditions. In spite of the progresses and achievements in the research on fullerenes and CNTs, industrial application of these novel materials is still totally lacking, and one of the reasons for this is undoubtedly the prohibitively high cost of producing fullerenes and CNTs. We thought that it is crucial to find a way of producing these novel carbon materials that will be used on an industrial scale to start the long awaited new technologies based on these novel materials in the future.

Since coals are cheap and abundant in China, with confirmed reserves of more than 1000 billion tons and an annual production capacity of about 1.4 billion tons, the Chinese coals could be used as starting materials to produce the high added value fullerenes and CNTs. For this purpose, a number of plasma arcing experiments have been carried out in our laboratory using carbon rods manufactured from Chinese coals to prepare fullerenes and carbon nanomaterials with high purity helium as buffer gas. Fullerenes were prepared at lower pressure of 20kPa, while carbon nanotubes were prepared at relatively higher pressure of 30kPa. It has been found that the composition of crude fullerenes obtained from different carbon rods made from coals differed from each other. There is a fairly good linear relationship between the C_{60}/C_{70} content in fullerenes and the volatile matter content in raw coals. As the volatile matter content increases, the C_{70} content in crude fullerenes increases while at the same time C_{60} content decreases. This means that relatively larger amounts C_{70} can be prepared from those young coals with a high volatile matter content. The highest C_{70}/C_{60} ratio in crude fullerene from one young Chinese coal is 38.9/59.0 that is more than two times higher than that from high purity graphite. In this paper we report that higher fullerenes such as C_{104} and C_{106} could also be obtained from the soot deposited on the inner walls of the reactor when CNTs, as the central part of a hard cylindrical deposit on the cathode, is prepared as the main target product. The favorable isomeric structures for these giant fullerenes are also predicted on the basis of the phason line criterion.

Experimental

Preparation of higher fullerenes

The manufacturing process for fullerenes from coals has been reported elsewhere[1]. In this paper fullerene soot was produced as the by-product of carbon nanotubes by the arc discharge method using coal-derived coke rods as anode with high purity helium as buffer gas while high purity graphite was used as the cathode. The weight of the graphite electrode remained the same before and after the

* Author to whom correspondence should be addressed, E-mail: jqiu@chem.dlut.edu.cn

arcing experiments, which suggests that the graphite cathode is not consumed during the arcing vaporization process. A voltage of 30 V was used and a current of about 100 A was passed through the electrodes. After some time of operation, carbon nanotubes as the soft inner cores of the rod-like deposits on the cathode were formed while the soot containing higher fullerenes was deposited on the internal surfaces of the chamber. The preparation and characterization of CNTs will be discussed in another paper presented in this conference. The soot collected was first Soxhlet extracted with toluene and then washed with ether to obtain crude fullerenes.

The mass spectrum of the soot and the crude fullerenes were measured using a LD-TOF-MS (laser desorption time-of-flight mass spectrometry) (Shimadzu-Kratos, MALDI-III). The sample was mixed with a little amount of xylene and mounded on a stainless steel sample folder. On injecting N_2 laser pulse to the sample, fullerenes are evaporated and ionized. In this measurement, positive ion mode, reflectron type orbit is selected and 100 shots signals are averaged. Laser power is at about 80/90 level.

Prediction of favorable structures of higher fullerenes

It is well known that the number of IPR isomers for high fullerene molecule increases exponentially with the number of carbon atoms in the molecule. Thus, it is necessary to know which structure is the most favorable one for the higher fullerene molecule. Here we use a new method called the phason line[2,3] to study the relative stabilities of these higher fullerenes and to predict the extractable isomers. This is a difficult task because there are 823 IPR isomers for C_{104} and 1233 for C_{106} .

Results and Discussion

All of the crude fullerene samples and soot samples were analyzed using laser desorption time-of-flight mass spectrometry. For each sample, clear peaks of C_{60} , C_{70} and higher fullerenes are confirmed. Figure 1 shows a typical LD-TOF-MS spectra recorded of the crude fullerene materials from two different coals. It can be seen clearly that besides C_{60} and C_{70} , the higher fullerenes ions including C_{104} , C_{106} and C_{108} ions, which correspond to the most abundant higher fullerenes in the soot, give the most prominent peaks in the spectra.

Analysis of the remaining black toluene-insoluble materials and the soot materials by LD-TOF mass spectrometry shows that they also contain larger fullerenes in the range between C_{100} and C_{360} in addition to some residual C_{60} and C_{70} . It was reported that the giant or higher fullerenes of this size can be solubilized in high-boiling solvents like 1,2,4-tetra-methylbenzene (bp 214 °C) or 1,2,4,5-tetramethylbenzene (bp 197 °C). It should be noted that the giant fullerenes with carbon atom numbers up to

C_{400} could be prepared from graphite, PAHs and higher oxides of carbon, by a number of techniques including the laser vaporization technique, the resistive heating and the arc vaporization method.

Currently we are trying to isolate macroscopic quantities of these higher fullerenes with the number of carbon atoms over 100 following an experimental protocol for fullerene isolation and separation which was developed by Professors Francois Diederich and Robert L. Whetten at UCLA[4] but no success is achieved till this paper is written up. The separation and characterization of higher fullerenes offer enormous experimental difficulties and the fact that only a few particular isomers were selected by nature to form in the fullerene-containing soot from among the vast number of apparently similar structural isomers poses a challenging problem to us.

Once macroscopic quantities of higher fullerenes such as C_{104} is obtained, the structural analyses could be carried out via a number of physical methods including XRD and ^{13}C NMR which have been widely used to characterize a few isomers of smaller fullerenes C_{76} , C_{78} , C_{82} and C_{84} . The carbon-13 NMR information will allow us to compare the experimental data with those theoretically predicted structures. For the separable structures of higher fullerenes, two useful guidelines are commonly adopted as the criteria: (1) the isolated pentagon rule (IPR) is the necessary condition and (2) the determined structures agree with the most favorable ones predicted by energy calculations. The second guideline has been strengthened by the observation that the numbers of NMR signals exhibited by the extracted isomers have been consistent with those expected for the symmetries of the lowest-energy isomers. Unfortunately, at the moment the LD-TOF-MS is the only information we got about the higher fullerenes including C_{104} and C_{106} . Thus, we have to rely on theoretical studies such as the energy calculations to predict which structure is the most stable one for each giant fullerene molecule that can be extracted and further purified to produce large amounts of sample for physical analysis. It is clear that we need some practical means of selecting good structures from the large number of IPR isomers for the characterization of higher fullerenes such as C_{104} and C_{106} .

Several years ago, Osawa and his colleagues developed new stability criteria for selecting favorable isomers of fullerenes satisfying the isolated pentagon rule (IPR) based on a topological entity which was termed as the phason line, the phase boundary between the surface patches having different patterns of π conjugations. Their results were published in *Electron. J. Theor. Chem.*, 1, 163-171 (1996). Unfortunately, however, this journal from Wiley was discontinued, hence only a few libraries have the copies. They proposed two conditions for the stable structure among the IPR isomers that conform to isolated

pentagon rule: the absence of branching (node) and the longest possible length in the phason line. The presence of the phason line in the fullerene structure signifies disruption of continuous π conjugation and certain loss in de-localization energy. The branching of the phason line (node) means further disruptions and higher π energy. On the other hand, a relatively narrow stretch along the phason line has a decreased curvature, in which the steric strain due to skeletal deformation is partly relieved. Hence the longer the phason line, the lower the σ energy. In the higher fullerenes C_n , $76 \leq n < 100$, the latter criterion works well, which means that the skeletal strain is the decisive cause of stability ranking among the isomers. The failure to separate leapfrog fullerenes (those having perfectly continuous π conjugation and no phason line) in this size range is due to the steric effect. The distribution of pentagonal rings in the fullerene molecules can be well reflected by the location, length and branching of the phason line.

Here in this paper we apply the phason line criteria to fullerenes C_{104} and C_{106} that existed in the soot obtained while preparing CNTs from coal-derived carbon rods, as the MS spectrum in Fig. 1 revealed, for the following two purposes. One is to take advantage of the new theory developed by Osawa and his colleagues to predict extractable isomers for these giant fullerenes. Another purpose is to know at which size the giant fullerenes with leapfrog structures would acquire enough stability to be separated from other fullerenes, because it is expected that the skeletal deformation should be diminished in larger fullerenes such as C_{104} and C_{106} .

For all of the IPR isomers of C_{102} to C_{120} , the phason lines can be drawn on the net diagrams of these fullerene molecules. For the three higher fullerenes as shown in Table 1, 3855 net diagrams in total could be obtained. It has been found that the length criterion is of no use, only the zero-node criterion was used for selecting the favorable structures of these higher fullerenes. Leapfrog (no phason line) and carbon cylinder (one phason line) isomers were included in the selection (*vide infra*). Thus, for C_{104} , C_{106} and C_{108} fullerenes, about 15% of the total IPR isomers are left as the candidates for the favorable structures. It is believed that this level is loose enough to ensure safe coverage and yet still manageable for molecular mechanics evaluation.

MM3 geometry optimization was then performed on all of the 591 candidate structures selected. The distributions of the MM3 heats of formation values for each fullerene family were obtained. It was found that the value of the formation heat is in a relatively narrow range of about 50 kcal mol⁻¹ and the median values in the histograms shift towards the direction of lower energy, which indicate the appropriateness of our selection process.

The MM3 calculations allow us to give a primary stability ranking among the IPR isomers. Because of inherent uncertainty in the molecular mechanics ranking for fullerenes, Professor Osawa and his colleagues subjected the best ten from each of the C_{104} , C_{106} and C_{108} fullerenes to further geometry optimization with AM1/MOPAC semi-empirical MO method. Pertinent results of the MM3/AM1 calculations are summarized in Table 2. Despite the astoundingly large differences in the absolute values of the heats of formation between MM3 and AM1 as shown in Table 2, the agreements between the rankings are surprisingly good. With the LD-TOF mass spectrometry as the experimental information available now, Table 2 provides at the moment the only information on the likely candidates for extractable giant fullerenes. Global energy minimum for different fullerenes may appear to have outstanding stability (generally 3 kcal mol⁻¹) or more stable than the second most stable isomer. However, AM1 errors may be as large as 10 kcal mol⁻¹ and therefore we should not be concerned about this magnitude of energy difference.

It is clear from Table 2 that there is no particular preference for the symmetry among the low-energy structures. In all of the cases studied, the lowest point groups, C_1 and C_2 , occur most frequently, and highly symmetrical structures rarely appear in the list which is a contrast to that of the C_n fullerenes with $n < 100$. In other words, there is one outstanding stable single isomer with D_2 symmetry for C_{104} and two for C_{106} , both with C_s symmetry.

In the giant fullerenes studied here, leapfrog structures are expected in C_{108} . While no carbon cylinder appears in Table 2, the leapfrog structures do appear frequently. This suggests that aromatic stabilization due to the well-defined closed electronic configuration overrides the steric strain which dominated in the smaller leapfrog fullerenes up to C_{100} . This leads us to conclude that the regaining of the importance of stabilization may be general in giant C_n fullerenes with $n > 100$.

As discussed above, though the resurgence of stable leapfrog structures in larger fullerenes ($n > 100$) is stressed, not all leapfrogs in this range are especially stable, and this is very probably due to the steric reasons. So far, among the giant fullerenes studied, C_{120} has received the highest attention, and the often-studied D_{5d} - C_{120} is a leapfrog too, but it is at least 60 kcal mol⁻¹ less stable than the global minimum because of high skeletal strain arising from the narrow barrel shape.

Conclusions

Giant fullerenes such as C_{104} and C_{106} have been prepared from coal by arc evaporation method when carbon nanotubes deposited on the cathode as the central part of a hard cylindrical are produced as the main target product. The most stable structures of the giant fullerenes are predicted using the selection rules based on the concept of the phason line that was developed by Eiji Osawa and his colleagues in Japan. Of the two criteria, zero node and the longest possible total length of the phason line, both has been successfully used to predict the stability of smaller fullerenes, but only the first criterion works for giant fullerenes in which π electron configuration dominates the stability. In other words, in the case of giant fullerenes, the π electronic stability overrides the phason line length criterion and the round-shaped leapfrog structures appear to be the most stable structures.

References

[1] Qiu JS, Zhou Y, Yang ZG, Wang DK, Guo SC, Tsang SC and Harris PJF. *Fuel* 2000; 79:1303

- [2] Yoshida M, Fujita M, Goto H and Osawa E. *Electronic Journal of Theoretical Chemistry* 1996;1:151 (Note: this journal from Wiley was discontinued, now only a few libraries have the copies. Please contact Professor Eiji Osawa for the original copies.)
- [3] Yoshida M, Goto H, Hirose Y, Zhao X and Osawa E. *Electronic Journal of Theoretical Chemistry* 1996; 1:163
- [4] Diederich F and Whetten RL. *Acc. Chem. Res.* 1992; 25:119

Acknowledgements

This work was supported by the National Natural Science Foundation of China (grant No. 29976006) and the Natural Science Foundation of Liaoning Province, China (grant No. 95031 and No. 9810300701) and the Ministry of Education, China.

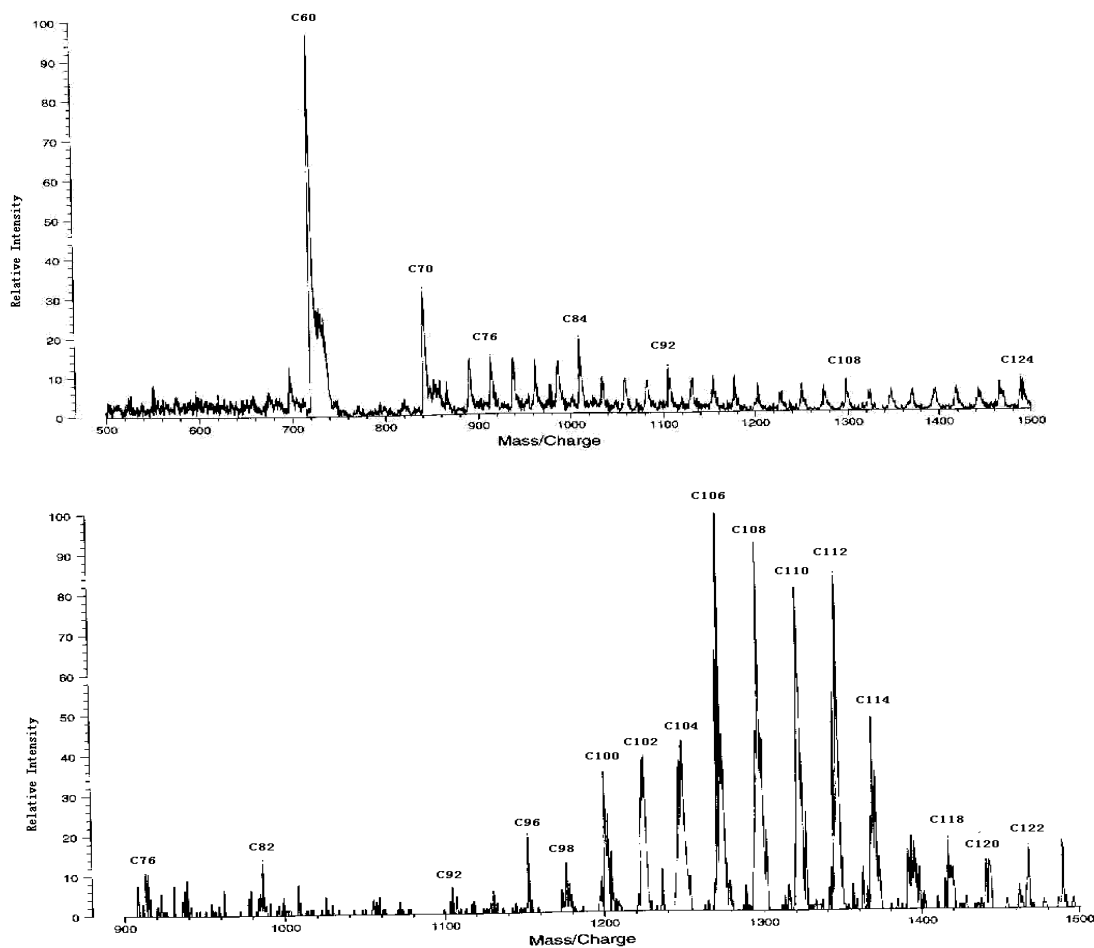


Figure 1 Typical mass spectra of coal-derived crude fullerenes measured by LD-TOF-MS (+mode, 100 shots averaged). (A) from Xiangyuan coal, (B) from Tonghua coal

Table 1. Total counts of IPR isomers (N) for C_{104} , C_{106} and C_{108} fullerenes, the number of isomers (N_o) having no phason line or no node in phason line and the percentage ratio (N_o/N)

n	N	N_o	Ratio
104	823	123	14.9
106	1233	187	15.2
108	1799	291	16.2

Table 2. Analysis of the ten best (MM3) isomers of C_{104} and C_{106} fullerenes

	RS N_o ^b	PG ^c	$L(N_p)$ ^d	MM3G2 ^a		Rank ^f	AM1	
				ΔH_f ^e	$\Delta\Delta H_f$		ΔH_f	$\Delta\Delta H_f$
C_{104}	812	D_2	22.4(1)	735.6	0.0	1	1311.2	0.0
	531	C_s	20.9(1)	737.8	2.2	2	1314.4	3.2
	238	C_2	19.4(1)	739.4	3.8	3	1315.3	4.1
	491	C_2	19.4(1)	739.7	4.1	4	1317.2	6.1
	99	C_1	19.4(1)	741.6	6.0	5	1318.9	7.8
	258	C_1	21.3(1)	741.8	6.2	6	1320.6	9.5
	492	C_1	26.1(1)	742.9	7.3	9	1322.9	11.7
	55	C_1	19.8(1)	743.2	7.6	8	1322.1	10.9
	97	C_2	26.5(1)	743.3	7.7	7	1320.9	9.8
	305	C_2	23.2(1)	743.5	7.9	10	1323.9	12.8
C_{106}	331	C_s	20.9(1)	742.8	0.0	1	1326.5	0.0
	189	C_s	15.0(1)	744.1	1.3	2	1327.0	0.6
	1031	C_2	22.4(1)	744.4	1.6	4	1330.6	4.2
	660	C_1	20.9(1)	745.3	2.5	6	1331.5	5.1
	318	C_1	22.8(1)	745.5	2.7	3	1330.5	4.1
	88	C_s	14.2(1)	746.2	3.4	8	1332.4	5.9
	221	C_1	14.2(1)	746.4	3.6	10	1334.0	7.5
	314	C_1	29.9(1)	746.7	3.9	5	1330.8	4.4
	220	C_1	28.4(2)	746.9	4.1	7	1332.0	5.6
	1030	C_1	29.5(2)	747.2	4.4	9	1333.6	7.1
C_{108}	206	D_{3h}	0.0(0)	741.3	0.0	1	1329.8	0.0
	1795	D_{6h}	0.0(0)	741.4	0.1	2	1334.3	4.6
	1698	C_s	15.0(1)	745.6	4.3	4	1339.0	9.2
	1771	D_2	22.4(1)	745.9	4.6	3	1336.2	6.5
	205	C_{2v}	0.0(0)	748.1	6.8	9	1346.8	17.1
	1497	C_1	24.3(1)	748.4	7.1	6	1340.8	11.0
	1686	C_2	38.8(1)	749.3	8.0	7	1342.3	12.5
	1796	D_{2d}	0.0(0)	749.4	8.1	10	1351.2	21.5
	1765	C_2	34.4(2)	749.5	8.2	5	1339.1	9.4
	1696	C_{2h}	30.0(1)	749.7	8.4	8	1344.1	14.4

^a A local version of MM3 updated for use on fullerenes.

^b Ring spiral sequential number.

^c Point group.

^d Total length and (number) of phason lines.

^e Heat of formation, kcal mol⁻¹.

^f AM1 energy ranking. Entries are sorted according to the MM3 energy rank.